

**Effect of probucol on cell proliferation in human ovarian cancer cells**

Journal:	<i>Toxicology Research</i>
Manuscript ID	TX-ART-03-2015-000088.R2
Article Type:	Paper
Date Submitted by the Author:	03-Nov-2015
Complete List of Authors:	Chuang, Lea-Yea; Kaohsiung Medical University, Biochemistry Guh, Jinn-Yuh; Kaohsiung Medical University, Internal Medicine Ye, Yi-Ling; National Formosa University, Biotechnology Lee, Ying-Ho; Chung Hwa University of Medical Technology, Biological Science and Technology Huang, Jau-Shyang; Chung Hwa University of Medical Technology, Biological Science and Technology

1
2
3
4
5
6
7
8
9
10
11
12
13
14
15
16
17
18
19
20
21
22
23
24
25
26
27
28
29
30
31
32
33
34
35
36

Effect of Probucol on Cell Proliferation in Human Ovarian Cancer Cells

Lea-Yea Chuang,^{a,*} Jinn-Yuh Guh,^{b,*} Yi-Ling Ye,^c Ying-Ho Lee,^d and Jau-Shyang Huang^{d,**}

^aDepartment of Biochemistry, Kaohsiung Medical University, Kaohsiung, Taiwan

^bDepartment of Internal Medicine, Kaohsiung Medical University, Kaohsiung, Taiwan

^cDepartment of Biotechnology, National Formosa University, Yunlin, Taiwan

^dDepartment of Biological Science and Technology, Chung Hwa University of Medical Technology,
Tainan, Taiwan

*Lea-Yea Chuang and Jinn-Yuh Guh contributed equally to this work.

**Corresponding author:

Jau-Shyang Huang

Department of Biological Science and Technology

Chung Hwa University of Medical Technology

Tainan, Taiwan, ROC

Tel: 886-6-2674567-420

Fax: 886-6-2675047

E-mail: jaushyang12@hotmail.com

Word count of abstract: 230

Total number of figures: 8

Total number of tables: 0

37
38
39
40
41
42
43
44
45
46
47
48
49
50
51
52
53
54
55
56
57
58
59
60
61
62
63

Abstract

Probucol is considered to be an important agent in promoting anti-oxidative action and protecting against tissue injury. However, little is known about the effect of probucol on the progression of ovarian carcinoma. The aim of this study was to investigate the effect of probucol on cellular proliferation in human ovarian cancer cells (PA-1 and SKOV-3) and explore the anti-proliferative mechanism of probucol in these cells. We found that probucol decreased cell growth in PA-1 and SKOV-3 cells in a dose-dependent manner. Treatment with probucol had no effect on cytotoxicity, the percentages of Annexin V-FITC positive cells and caspase-3 activity when compared with the vehicle group. No significant differences in the protein expression of Bcl-2 and cytochrome c, both of which were markers of cells undergoing apoptosis. Inhibition of cellular proliferation by probucol was caused by G1-phase arrest through regulating proteins associated with cell cycle progression, such as cyclin D1, p21^{Waf1/Cip1}, and p27^{Kip1}. Further study revealed that probucol strongly impaired the phosphorylation of IκBα and the nuclear translocation of NF-κB (p65). It also suppressed activation of ERK/JNK/p38 MAPK signaling. Moreover, the NF-κB inhibitor (PDTC), the ERK inhibitor (PD98059), the JNK inhibitor (SP600125), and the p38 MAPK inhibitor (SB203580) markedly attenuated cell growth of these cells. Our results indicate that probucol induces anti-proliferative effect via blocking of cell cycle progression and inactivation of NF-κB and MAPK pathways in human ovarian cancer cells.

64
65
66
67
68
69
70
71
72
73
74
75
76
77
78
79
80
81
82
83
84
85
86
87
88
89
90

Key words: ovarian cancer; probucol; proliferation; NF- κ B; MAPK; cell cycle.

Abbreviations: ERK, extracellular signal regulated kinase; I κ B α , inhibitory kappa B alpha; JNK, c-Jun N-terminal kinase; LDH, lactate dehydrogenase; MAPK, mitogen-activated protein kinase; NF- κ B, nuclear factor-kappaB; PCNA, proliferating cell nuclear antigen; PDTC, pyrrolidine dithiocarbamate; STS, staurosporine.

91 Introduction

92

93 ProbucoI is a diphenolic compound with anti-hyperlipidemic, anti-oxidative, anti-diabetic, and
94 anti-inflammatory properties that reduces tissue injury and histopathological changes.¹⁻⁶ It has a long
95 history of clinical application with established efficacy and safety profiles.^{2,3} Previous studies have
96 demonstrated that probucoI has diverse pharmacological properties with therapeutic effects on
97 cardiovascular and metabolic diseases.⁴⁻⁸ It can also modulate toxic promoting effect and can serve as a
98 potent chemopreventive agent to suppress oxidant induced tissue injury.^{2,4,8} Therefore, probucoI is
99 supposed to be an excellent agent in enhancing endogenous antioxidant reserve and protecting against
100 augmented oxidative stress.¹⁻⁴

101

102 Ovarian cancer is the deadliest of all gynecologic malignancies in many countries.⁹⁻¹¹ Because this
103 disease is nonspecific or asymptomatic at the early stage of its progression, the majority of ovarian
104 carcinoma patients are diagnosed with advanced stage disease.¹⁰⁻¹² For the therapy of ovarian carcinoma,
105 cytoreductive surgery and combination chemotherapies are standard strategies.¹³⁻¹⁶ However, tumor
106 relapse and the development of drug-resistant disease are still a knotty problem to be resolved in ovarian
107 carcinoma treatment.

108

109 It is well documented that oxidative stress modulates cell growth or genomic stability in both
110 physiological and pathophysiological conditions.¹⁷⁻¹⁹ Recent molecular and pathological evidences
111 suggest that in progressive stages of ovarian carcinoma, the oxidative stress can contribute to the
112 uncontrolled tumor expansion.^{18,19} Antioxidants, when added adjunctively, to first-line chemotherapy, may
113 improve the efficacy of cancer therapy.^{19,20} More recent data showed that probucoI was a potent
114 antioxidant that can serve as a powerful chemopreventive agent to suppress oxidant induced tissue injury
115 and carcinogenesis, in addition to being a cholesterol reducing and anti-atherogenic drug.²¹⁻²³ ProbucoI
116 exposure modulated iron nitrilotriacetate-dependent renal carcinogenesis and hyperproliferative
117 response.²³ It can induce anti-angiogenesis and apoptosis in athymic nude mouse xenografted human head

118 and neck squamous carcinoma cells.²⁴ On the other hand, probucol was able to activate NAD(P)H:quinone
119 reductase, one of the main detoxifying enzymes, and could then reduce chemical carcinogenesis and
120 toxicity.²⁵ Nanoassembly of probucol enabled novel therapeutic efficacy in the suppression of lung
121 metastasis of breast cancer.²⁶ Nevertheless, its potential effect on the progression of ovarian cancer has not
122 been explored yet.

123

124 It has been reported that nuclear factor-kappa B (NF- κ B) plays an important role in cellular redox
125 system in various cells.²⁷⁻²⁹ In unstimulated cells, the NF- κ B p50/p65 heterodimer is maintained in the
126 cytoplasm by binding to I κ B α . Upon stimulation, NF- κ B dissociates from I κ B α , translocates to the
127 nucleus, activates target genes and regulates diverse cellular functions.^{28,29} Most of the effects of NF- κ B
128 activation on cancer cells have been linked with cancer development and poor outcomes.^{30,31} Cancer cells
129 have been shown to exhibit a constitutively hyperactivated NF- κ B survival signaling pathways.³¹ Indeed,
130 aberrant regulation of NF- κ B pathway is believed to be a major event contributing to malignant
131 transformation and progression of ovarian cancer.^{32,33}

132

133 In this study, we hypothesized that probucol maybe is an effective candidate for antiovarian cancer
134 cells. Therefore, to examine this hypothesis, we investigated the inhibitory effects of probucol on cell
135 proliferation in human ovarian cancer PA-1 and SKOV-3 cells and its underlying molecular mechanism
136 for probucol-mediated cell cycle progression and NF- κ B signaling. We also identified signaling molecules
137 underlying probucol-modulated cell growth in in the two cell lines. Finally, our study displayed the
138 potential role of probucol in ovarian carcinoma chemotherapy or chemoprevention.

139

140

141

142

143

144

145 **Materials and methods**

146

147 **Reagents**

148 Anti-ERK1/2, -JNK, -p38 MAPK, -p21^{Waf1/Cip1}, -p27^{Kip1}, -Bcl-2, -c-Myc, -cytochrome c, -cdk4, -cyclin D1,
149 -PCNA, -p65, and -I κ B α antibodies were purchased from Santa Cruz Biotechnology, Inc, Santa Cruz, CA.
150 Anti-phospho-I κ B α , -phospho-ERK1/2, -phospho-JNK, -phospho-p38 MAPK, and Histone H3 antibodies
151 were obtained from Abcam, Cambridge, MA. HRP-conjugated goat anti-rabbit or anti-mouse secondary
152 antibody, streptavidin-peroxidase, and the enhanced chemiluminescence kit were obtained from
153 Amersham Corp, Arlington Heights, IL. Lactate dehydrogenase (LDH)-cytotoxicity assay kit was
154 purchased from BioVision, Mountain View, CA. PD98059, SP600125, and SB203580 was purchased from
155 Calbiochem, La Jolla, CA. N,N'-methylenebisacrylamide, acrylamide, SDS, ammonium persulfate, Temed,
156 and Tween 20 were purchased from Bio-Rad Laboratories, Hercules, CA. FBS, DMEM, antibiotics,
157 molecular weight standards, trypsin-EDTA, trypan blue dye, and all medium additives were obtained from
158 Life Technologies, Gaithersburg, MD. Probucol, staurosporine, dimethyl sulfoxide (DMSO), pyrrolidine
159 dithiocarbamate (PDTC), propidium iodide (PI), 3-(4,5-dimethylthiazol-2-yl)-2,5-diphenyl tetrazolium
160 bromide (MTT) colorimetric assay kit, Annexin V-FITC apoptosis detection kit, caspase-3 activity assay
161 kit, and anti- β -actin antibodies, and all other chemicals were purchased from Sigma-Aldrich Chemical, St.
162 Louis, MO.

163

164 **Culture conditions**

165 The human ovarian cancer cell lines (PA-1 and SKOV-3) were obtained from the American Type Culture
166 Collection (Manassas, VA, USA). These cells were grown in culture flasks (Nunclon, Denmark) and
167 maintained in DMEM supplemented with 100 i.u./ml penicillin, 100 μ g/ml streptomycin and 10% FBS in
168 a humidified 5% CO₂ incubator at 37°C. In this study, cells were exposed to serum-free (0.1% FBS)
169 DMEM supplemented with probucol or probucol's vehicle (0.05% DMSO) for 4 h prior to timed exposure
170 to DMEM containing 10% FBS. For cell number analysis, cells (1.2×10^5 cells per well) were seeded in
171 6-well (9.6 cm²/well) culture plates (Nunclon) and grown in the added test agents. Subconfluent cells were

172 harvested by using 0.25% trypsin-EDTA. Cells were resuspended in equal volumes of medium and trypan
173 blue (0.05% solution) and counted using a haemocytometer. Trypan blue dye exclusion was used to assess
174 cell viability. Each experimental data point represents the mean of duplicate wells from three independent
175 experiments.

176

177 **Cell viability assay**

178 Cell viability (MTT) assay was performed to evaluate the proliferation of PA-1 and SKOV-3 cells. Cells
179 were plated and incubated for 24 h in wells of a 96-well plate. Then probucol (5, 10, 50, 100, 500 μ M) and
180 vehicle (0.05% DMSO) were added to the wells. Cells with no added treatment were used as control. After
181 treatment, 10 μ l of sterile MTT dye was added to each well, and the cells were incubated for 6 h at 37°C.
182 Then 100 μ l of acidic isopropanol (0.04 M HCl in isopropanol) were added and thoroughly mixed.
183 Spectrometric absorbance at 595 nm (for formazan dye) was measured with the absorbance at 655 nm for
184 reference. According to cell viability assay and cell number analysis, the lower and non-toxic
185 concentration of probucol (100 μ M) is used in subsequent experiments.

186

187 **Cytotoxicity assay**

188 LDH content was determined by using an LDH-cytotoxicity assay kit, which is based on a coupled
189 enzymatic reaction that results in the conversion of a tetrazolium salt into a red formazan product. The
190 increase in the amount of formazan produced in culture supernatant directly correlates with the increase in
191 the number of lysed cells. The formazan was quantified spectrophotometrically by measuring its
192 absorbance at 490 nm. A group of wells were treated with 1% Triton X-100 solution for maximum LDH
193 release. The mean of the background value was subtracted from all other values. Cytotoxicity in
194 experimental samples expressed as a percentage of the LDH release of 10% FBS-treated cells (control).

195

196 **Caspase-3 activity assay**

197 Caspase-3 activity was measured using a colorimetric activity kit as per the manufacturer's instructions.

198 This assay measures the hydrolysis of acetyl-Asp-Glu-Val-Asp p-nitroanilide (Ac-DEVD-pNA) by
199 caspase-3 that results in the release of p-nitroanilide (pNA). Absorbances were measured at 405 nm and
200 the results calculated using a standard curve derived from known concentrations of pNA.

201

202 **Western blotting**

203 One day before treatment, 1.5×10^6 cells were seeded in T-75 flasks. Cell growth medium was replaced
204 24 h after seeding, followed by addition of test compounds after medium change. For protein analysis,
205 total cell lysates were harvested and lysed in 1 × SDS-polyacrylamide gel electrophoresis (SDS-PAGE)
206 sample buffer (0.375 M Tris-HCl, pH 6.8, 30% glycerol, 10% SDS, 2% β-mercaptoethanol, 0.1%
207 bromophenol blue), and heated for 3 min at 95°C. Samples were resolved by 10% SDS-PAGE, and then
208 transferred to Protran membranes (0.45 μm, Schieicher & Schuell, Keene, NH, USA). The membranes
209 were blocked in blocking solution and subsequently probed with primary antibodies. The membrane was
210 incubated in 4000× diluted HRP-conjugated goat anti-rabbit or anti-mouse secondary antibody. The
211 protein bands were detected using the enhanced chemiluminescence (ECL) system. For the NF-κB and
212 ERK/JNK/p38 MAPK activation assay, proteins were resolved by SDS-PAGE and transferred to Protran
213 membranes. The membranes were probed with anti-phospho-IκBα (1 μg/ml), anti-phospho-ERK1/2 (1
214 μg/ml), anti-phospho-JNK (1 μg/ml), anti-phospho-p38 MAPK (1 μg/ml), anti-IκBα (1 μg/ml),
215 anti-ERK1/2 (0.75 μg/ml), anti-JNK (1 μg/ml), and anti-p38 MAPK (0.75 μg/ml) antibodies.
216 Immunoreactive proteins were detected with the ECL system as described above. The intensity of Western
217 blot bands was quantified by densitometric analysis. Results were expressed as the ratio of intensity of the
218 protein of interest to that of β-actin or the indicated protein from the same sample.

219

220 **Assay of cytochrome c release**

221 To obtain cytosolic fractions, cells were harvested and washed once in cold PBS, and then incubated with
222 mitochondria isolation buffer (300 mM sucrose, 10 mM KCl, 1.5 mM MgCl₂, 20 mM HEPES, 1 mM
223 EDTA, 1 mM EGTA, 1 mM DTT, 1 mM PMSF, 1 μg/ml leupeptin, 10 μg/ml pepstatin, 10 μg/ml
224 aprotinin) on ice for 30 min. Then, cells were disrupted by 20 passages through 26-gauge needle. The

225 disrupted cells were centrifuged at $750 \times g$ for 10 min at 4 °C. The resulting supernatant was then twice
226 centrifuged at $12,000 \times g$ for 20 min at 4 °C, and the supernatant was collected as the cytosolic fraction.
227 For assay of cytochrome c release, the cytosolic fraction was electrophoresed on 12% SDS-PAGE, and
228 Western blot was then performed using anti-cytochrome c antibody.

229

230 **Cell cycle analysis and Annexin V staining assay**

231 Relative cell size and DNA content were assessed by flow-cytometric analysis. At various time points,
232 cells were harvested and fixed with 100% ethanol and then placed at -20°C for overnight. After fixation,
233 cells were centrifuged and washed once with PBS containing 1% bovine serum albumin. For staining with
234 DNA dye, cells were resuspended in 0.5 to 1 ml of PI solution containing RNase and incubated at 37°C for
235 30 min, followed by overnight incubation at 4°C . For Annexin V staining, 1×10^4 cells were collected and
236 stained with Annexin V-FITC according to the manufacturer's instruction. The PI and Annexin V stained
237 cells were collected and analyzed using BD flow-cytometry systems. The percentage of Annexin V-FITC
238 positive cells was considered as the percentage of apoptotic cells.

239

240 **Statistical analysis**

241 Analysis and graphing of data were performed with Prism 3.0 (GraphPad Software, San Diego, CA). Data
242 are expressed as means \pm SEM. Statistical analysis was performed by ANOVA for multiple group
243 comparison and by Student's t-test for direct comparison of two groups. P values <0.05 were considered
244 significant.

245

246

247

248

249

250

251 **Results and discussion**

252

253 **Effect of probucol on proliferation in human ovarian cancer cells**

254 To determine whether probucol modulated cellular proliferation in human ovarian cancer cell lines (PA-1
255 and SKOV-3), cells were seeded in culture plates in equal numbers and left to grow to 30 to 40%
256 confluence in medium containing 10% FBS. Cells were washed twice with PBS buffer and maintained in
257 medium containing 0.1% FBS for 48 h. The growth-arrested cells were then treated with probucol or
258 probucol's vehicle (0.05% DMSO) in the presence of 10% FBS for 3 d. As shown in Fig. 1, raising the
259 ambient probucol concentration (5, 10, 50, 100, 500 μM) causes a dose-dependent decrease in cell
260 viability (Fig. 1a) and cell number (Fig. 1b) when compared with control (10% FBS) or probucol's vehicle
261 in PA-1 and SKOV-3 cells. The high concentrations (100 μM and 500 μM) of probucol cause significantly
262 decrease in cellular mitogenesis when compared with control or vehicle. In addition, the effects of
263 probucol and the cytotoxic-inducer staurosporine on the membrane integrity and cytotoxicity of these cells
264 were also clarified through evaluating the release of LDH into the experimental medium. We found that
265 staurosporine (0.1 μM) and probucol (500 μM) promoted the LDH release when compared with control
266 (Fig. 1c). According to cell viability assay and cell number analysis, the lower and non-toxic concentration
267 of probucol (100 μM) was used in subsequent experiments.

268

269 **Effect of probucol on apoptosis in human ovarian cancer cells**

270 In order to assess whether probucol inhibited cellular proliferation through an apoptotic mechanism, we
271 analyzed in detail changes in expression of the anti-apoptotic protein Bcl-2 and the apoptogenic protein
272 cytochrome c and caspase-3. As shown in Fig. 2a and 2b, probucol (100 μM) treatments had no obvious
273 effect on Bcl-2 and cytosolic cytochrome c expression as compared with control or vehicle in PA-1 and
274 SKOV-3 cells. However, the pronounced decrease in Bcl-2 and increase in cytosolic cytochrome c were
275 detected after the apoptotic-inducer staurosporine (0.1 μM) treatment. Furthermore, no obviously
276 differences were observed regarding the percentages of Annexin V-FITC positive cells (Fig. 2c) and the
277 caspase-3 activation (Fig. 2d) between probucol (100 μM) and control cultures in these cells. However,

278 staurosporine did markedly increase apoptotic cells and caspase-3 activity.

279

280 Indeed, probucol has been demonstrated to modulate cell proliferation and cytotoxicity in many
281 tissues and organs.⁵⁻⁷ It regulates programmed cell death and exerts both agonistic and antagonistic effects
282 on apoptotic signaling.^{24,25,34} Some lines of evidence have indicated that probucol increased the expression
283 of anti-apoptotic protein and reduced apoptosis. It attenuates cyclophosphamide-induced oxidative
284 apoptosis, p53 and Bax signal expression in rat cardiac tissues.³⁵ Pretreatment with probucol significantly
285 blocked apoptosis and increased the expression of Bcl-2 protein in human umbilical vein endothelial
286 cells.³⁶ It also inhibited the lipopolysaccharide-reduced expression of Bcl-2 protein and then suppressed
287 apoptosis in vascular smooth muscle cells.³⁷ Additionally, it could protect renal proximal tubular cells
288 from methylguanidine-induced apoptosis.³⁸ Nevertheless, in the present study, we found that probucol did
289 not alter the cytotoxicity, the percentages of Annexin V-FITC positive cells and caspase-3 activation in
290 human ovarian cancer cells. Moreover, it had no significant effect on Bcl-2 and cytosolic cytochrome c
291 expression. Because probucol did not modulate apoptosis and cytotoxicity, our findings strongly suggest
292 that it probably exerted its anti-proliferative effect by inhibiting cell cycle progression in these cells.

293

294 **Effects of probucol on cell cycle regulatory molecules and cell cycle progression**

295 To gain further insight into the mechanism exerted by probucol, we next wished to determine whether
296 probucol is responsible for inhibition of cell cycle progression in human ovarian cancer cells. Western blot
297 analysis revealed that probucol (100 μ M) can not affect protein synthesis of cdk4 and c-Myc (Figs. 3a and
298 3b) in PA-1 and SKOV-3 cells. However, probucol clearly reduced protein synthesis of cyclin D1 and
299 PCNA. Interestingly, protein levels of p27^{Kip1} and p21^{Waf1/Cip1} were significantly induced by probucol.
300 Furthermore, flow-cytometric analysis showed that the percentages of cells in G0/G1 phase increased
301 while the percentages of cells in G2/M phase decreased in the probucol-treated cells compared with the
302 control groups (Fig. 4). These results indicated that suppression of cyclin D1 and PCNA and induction of
303 p21^{Waf1/Cip1} and p27^{Kip1} are the underlying mechanisms by probucol to promote inhibition of cell cycle
304 progression in human ovarian cancer cells.

305

306 **Effects of probucol and some kinase inhibitors on NF- κ B and ERK/JNK/p38 MAPK activation in**
307 **human ovarian cancer cells**

308 Evidence is accumulating to indicate that the NF- κ B signaling pathway may be an important feature of
309 ovarian carcinoma.^{32,33,39} To investigate whether probucol and the NF- κ B signaling pathway played roles
310 in ovarian cancer cell proliferation, probucol and the NF- κ B inhibitor PDTC were used to pretreat PA-1
311 and SKOV-3 cells. We found that phospho-I κ B α and nuclear p65 were strongly reduced by probucol
312 treatment while protein levels of I κ B α and cytosolic p65 were enhanced (Figs. 5a and 5b). In addition,
313 phosphorylation of I κ B α was markedly attenuated by administration of PDTC (10 μ M).

314

315 To clarify whether the ERK/JNK/p38 MAPK pathway played a role in cell growth, the ERK kinase
316 inhibitor PD98059, the JNK kinase inhibitor SP60012, and the p38 MAPK kinase inhibitor SB203580
317 were used to pretreat PA-1 and SKOV-3 cells. After exposure of cultured cells to probucol and kinase
318 inhibitors for 12 h, we found that probucol significantly reduced phospho-ERK, phospho-JNK and
319 phospho-p38 MAPK without obviously affecting ERK, JNK and p38 MAPK protein levels (Fig. 6a–c).
320 Phosphorylation of ERK, JNK and p38 MAPK were significantly reduced by administration of PD98059
321 (10 μ M), SP600125 (5 μ M), and SB203580 (5 μ M), respectively. On the other hand, we further examined
322 the effects of PDTC, PD98059, SP600125, and SB203580 on cell viability and cell numbers in PA-1 and
323 SKOV-3 cells. As depicted in Fig. 7, compared with the control groups, growth inhibition were clearly
324 observed in these cells treated with probucol (100 μ M), PDTC (10 μ M), PD98059 (10 μ M), SP600125 (5
325 μ M), and SB203580 (5 μ M). Additionally, growth inhibition was enhanced by probucol plus each kinase
326 inhibitors in these cells. These results indicated that down-regulation of the NF- κ B and ERK/JNK/p38
327 MAPK signaling pathways are important mechanisms by probucol to promote inhibition of cellular
328 proliferation in human ovarian cancer cells.

329

330 To further evaluate whether NF- κ B and ERK/JNK/p38 MAPK pathways mediate cellular
331 mitogenesis of PA-1 and SKOV-3 cells, we first knockdown of p65, ERK, JNK and p38 MAPK by

332 specific siRNAs, as shown in Supplemental Figure 1, these protein levels in silenced cells were decreased
333 significantly than those in non-silencing RNA cells, confirming successfully silenced p65, ERK, JNK and
334 p38 MAPK in these cells. Also in these cases, knockdown of ERK, JNK and p38 MAPK strongly reduced
335 phosphorylation of ERK, JNK and p38 MAPK, respectively. We then investigated the effects of probucol,
336 p65 siRNA, ERK siRNA, JNK siRNA and p38 MAPK siRNA on cellular mitogenesis in PA-1 and
337 SKOV-3 cells. Supplemental Figure 2 showed that knockdown of p65, ERK, JNK and p38 MAPK by
338 specific siRNAs caused marked drop in cell viability and cell numbers further implicate the involvement
339 of NF- κ B and ERK/JNK/p38 MAPK pathways in growth control. Additionally, growth inhibition was
340 enhanced by probucol plus each kinase inhibitors in these cells. Taken together, these results suggested
341 that probucol down-regulates cellular proliferation through NF- κ B and ERK/JNK/p38 MAPK pathways.

342

343 Several reports have indicated that both the NF- κ B and MAPK signaling pathways play important
344 roles in cell proliferation, differentiation, transformation, apoptosis, and the regulation of a variety of
345 transcription factors and gene expressions.⁴⁰⁻⁴³ Inactivation of the NF- κ B and MAPK signaling pathways
346 are involved in anti-oxidative effects under various pathological conditions.^{28,42-44} Recent studies have
347 implied that probucol may decrease NF- κ B or MAPK activation and exert its unique pharmacologic
348 actions and protective effects in many tissues and organs.^{45,46} In human aortic endothelial cells, probucol
349 could suppress the activation of NF- κ B and inhibit endothelial apoptosis.⁴⁶ Besides, probucol reversed
350 adriamycin-induced cardiomyopathy by inhibiting the ERK/JNK/p38 MAPK pathway via diminishing
351 oxidative stress.⁴⁷ In the current results, probucol treatment displayed a marked decrease in cell viability
352 through inhibiting the NF- κ B and ERK/JNK/p38 MAPK pathways in human ovarian cancer cells. This
353 suggests that probucol is able to inhibit cell growth, one of the main features acquired by downregulation
354 of NF- κ B and ERK/JNK/p38 MAPK signaling, and could then reduce proliferative potential of ovarian
355 cancers.

356

357

358

359 Conclusions

360

361 In conclusion, the present work explains the mechanism of action of probucol that modulates proliferation
362 and cell cycle progression in human ovarian cancer cells (Fig. 8). We found that probucol caused
363 inhibition of cellular proliferation partly by obstructing of cell cycle progression in two human ovarian
364 cancer cell lines—PA-1 and SKOV-3. However, no apparent apoptosis was evident in any of the cell lines.
365 The model suggested in Fig. 8 demonstrates that the ability of probucol to induce cell cycle arrest was
366 verified by the observation that it significantly decreased protein expression of cyclin D1 and PCNA but
367 increased protein levels of p21^{Waf1/Cip1} and p27^{Kip1}. Exposure of probucol also attenuated NF-κB and
368 ERK/JNK/p38 MAPK activation. On the other hand, the specific inhibitors (e.g., PDTC, PD98059,
369 SP600125, and SB203580) significantly inhibited cellular growth in these cells. Overall, this is the first
370 report suggesting that probucol has the potent inhibitory effect against human ovarian cancer cell
371 proliferation, and NF-κB and ERK/JNK/p38 MAPK pathways may be important targets of probucol (Fig.
372 8). Blockade of these signaling pathways by probucol may be an effective strategy in the treatment of
373 ovarian cancers.

374

375

376

377

378

379

380

381

382

383

384

385

386

387

388 **Acknowledgment**

389

390 This work was supported by Research Grants (NSC-102-2314-B273-001 to J-S Huang) from the National
391 Science Council, Republic of China.

392

393

394

395 *The authors have declared no conflict of interest.*

396

397

398

399

400

401

402

403

404

405

406

407

408

409

410

411

412

413

414 **Notes and references**

415

- 416 1 A. Adameova, Y. J. Xu, T. A. Duhamel, P. S. Tappia, L. Shan and N. S. Dhalla, *Curr. Pharm. Des.*,
417 2009, **15**, 3094–3107.
- 418 2 S. Yamashita and Y. Matsuzawa, *Atherosclerosis*, 2009, **207**, 16–23.
- 419 3 D. Tanous, N. Hime and R. Stocker, *Redox. Rep.*, 2008, **13**, 48–59.
- 420 4 R. Stocker, *Curr. Opin. Lipidol.*, 2009, **20**, 227–235.
- 421 5 J. W. Heinecke, *J. Exp. Med.*, 2006, **203**, 813–816.
- 422 6 S. P. Moubayed, T. M. Heinonen and J. C. Tardif, *Curr. Opin. Lipidol.*, 2007, **18**, 638–644.
- 423 7 M. T. Saleem, M. C. Chetty and S. Kavimani, *Ther. Adv. Cardiovasc. Dis.*, 2014, **8**, 4–11.
- 424 8 J. R. Walker, A. Sharma, M. Lytwyn, S. Bohonis, J. Thliveris, P. K. Singal and D. S. Jassal, *J. Am. Soc.*
425 *Echocardiogr.*, 2011, **24**, 699–705.
- 426 9 P. S. Munksgaard and J. Blaakaer, *Gynecol. Oncol.*, 2012, **124**, 164–169.
- 427 10 Z. Stanojevic, B. Djordjevic, S. B. Pajovic, J. Zivanov-Curlis and S. Najman, *J. BUON.*, 2009, **14**,
428 7–18.
- 429 11 R. Longuespée, C. Boyon, A. Desmons, D. Vinatier, E. Leblanc, I. Farré, M. Wisztorski, K. Ly, F.
430 D'Anjou, R. Day, I. Fournier and M. Salzet, *Cancer Metastasis Rev.*, 2012, **31**, 713–732.
- 431 12 L. Batista, T. Gruosso and F. Mechta-Grigoriou, *Int. J. Biochem. Cell Biol.*, 2013, **45**, 1092–1098.
- 432 13 M. Fung-Kee-Fung, T. Oliver, L. Elit, A. Oza, H. W. Hirte and P. Bryson, *Curr. Oncol.*, 2007, **14**,
433 195–208.
- 434 14 J. Liu and U. A. Matulonis, *Clin. Cancer Res.*, 2014, **20**, 5150–5156.
- 435 15 S. Banerjee and M. Gore, *Oncologist*, 2009, **14**, 706–716.
- 436 16 A. A. Secord, A. B. Nixon and H. I. Hurwitz, *Gynecol. Oncol.*, 2014, **135**, 349–358.
- 437 17 W. C. Burhans and N. H. Heintz, *Free Radic. Biol. Med.*, 2009, **47**, 1282–1293.
- 438 18 J. Chiu and I. W. Dawes, *Trends. Cell Biol.*, 2012, **22**, 592–601.
- 439 19 M. Tertilt, A. Jozkowicz and J. Dulak, *Curr. Pharm. Des.*, 2010, **16**, 3877–3894.
- 440 20 P. Rajendran, N. Nandakumar, T. Rengarajan, R. Palaniswami, E. N. Gnanadhas, U. Lakshminarasiah,
441 J. Gopas and I. Nishigaki, *Clin. Chim. Acta*, 2014, **436**, 332–347.
- 442 21 E. el-Demerdash, E. D. el-Denshary, M. el-Didi, N. Al-Gharabli and A. M. Osman, *Anticancer Res.*,
443 2002, **22**, 977–984.
- 444 22 M. Zarkovic, X. Qin, Y. Nakatsuru, S. Zhang, Y. Yamazaki, H. Oda, T. Ishikawa and T. Ishikawa,
445 *Carcinogenesis*, 1995, **16**, 2599–2601.
- 446 23 M. Iqbal, Y. Okazaki and S. Okada, *Mol. Cell. Biochem.*, 2007, **304**, 61–69.
- 447 24 G. Nishimura, S. Yanoma, H. Mizuno, K. Kawakami and M. Tsukuda, *Jpn. J. Cancer Res.*, 1999, **90**,
448 1224–1230.
- 449 25 M. Iqbal and S. Okada, *Pharmacol. Toxicol.*, 2003, **93**, 259–263.
- 450 26 Z. Zhang, H. Cao, S. Jiang, Z. Liu, X. He, H. Yu and Y. Li, *Small*, 2014, **10**, 4735–4745.
- 451 27 A. Siomek, *Acta Biochim. Pol.*, 2011, **59**, 323–331.
- 452 28 M. J. Morgan and Z. G. Liu, *Cell Res.*, 2011, **21**, 103–115.
- 453 29 C. Pantano, N. L. Reynaert, A. Vliet and Y. M. Janssen-Heininger, *Antioxid. Redox. Signal.*, 2006, **8**,

- 454 1791–1806.
- 455 30 H. Jing and S. Lee, *Mol. Cells*, 2014, **37**, 189–195.
- 456 31 T. Okamoto, T. Sanda and K. Asamitsu, *Curr. Pharm. Des.*, 2007, **13**, 447–462.
- 457 32 A. E. Drummond and P. J. Fuller, *Mol. Cell. Endocrinol.*, 2012, **359**, 85–91.
- 458 33 K. L. White, D. N. Rider, K. R. Kalli, K. L. Knutson, G. P. Jarvik and E. L. Goode, *Cancer Causes*
459 *Control*, 2011, **22**, 785–801.
- 460 34 H. J. Oskarsson, L. Coppey, R. M. Weiss and W. G. Li, *Cardiovasc. Res.*, 2000, **45**, 679–687.
- 461 35 Y. A. Asiri, *Oxid. Med. Cell. Longev.*, 2010, **3**, 308–316.
- 462 36 Z. Dai, D. F. Liao, D. J. Jiang, H. W. Deng and Y. J. Li, *Naunyn Schmiedebergs Arch. Pharmacol.*,
463 2004, **370**, 314–319.
- 464 37 J. F. Li, S. Chen, J. D. Feng, M. Y. Zhang and X. X. Liu, *Exp. Mol. Pathol.*, 2014, **96**, 250–256.
- 465 38 F. Wang, B. Yang, G. H. Ling, C. Yao and Y. S. Jiang, *Ren. Fail.*, 2010, **32**, 978–985.
- 466 39 L. Hernandez, S. C. Hsu, B. Davidson, M. J. Birrer, E. C. Kohn and C. M. Annunziata, *Cancer Res.*,
467 2010, **70**, 4005–4014.
- 468 40 A. C. Ledoux and N. D. Perkins, *Biochem. Soc. Trans.*, 2014, **42**, 76–81.
- 469 41 E. K. Kim and E. J. Choi, *Biochim. Biophys. Acta*, 2010, **1802**, 396–405.
- 470 42 D. J. Erstad and J. C. Jr. Cusack, *Surg. Oncol. Clin. N. Am.*, 2013, **22**, 705–746.
- 471 43 E. F. Wagner and A. R. Nebreda, *Nat. Rev. Cancer*, 2009, **9**, 537–549.
- 472 44 E. D. Owuor and A. N. Kong, *Biochem. Pharmacol.*, 2002, **64**, 765–770.
- 473 45 M. Zhang, J. Wang, J. H. Liu, S. J. Chen, B. Zhen, C. H. Wang, H. He and C. X. Jiang, *Mol. Med. Rep.*,
474 2013, **7**, 177–182.
- 475 46 M. Aoki, T. Nata, R. Morishita, H. Matsushita, H. Nakagami, K. Yamamoto, K. Yamazaki, M.
476 Nakabayashi, T. Ogihara and Y. Kaneda, *Hypertension*, 2001, **38**, 48–55.
- 477 47 H. Lou, I. Danelisen and P. K. Singal, *Am. J. Physiol. Heart. Circ. Physiol.*, 2005, **288**, 1925–1930.
- 478
- 479
- 480
- 481
- 482
- 483
- 484
- 485
- 486
- 487

488 **Figure legends**

489

490 **Fig. 1** Effects of different concentrations of probucol on cellular mitogenesis and cytotoxicity in human
491 ovarian cancer cell lines (PA-1 and SKOV-3). Serum-deprived cells were treated with 10% FBS (control),
492 probucol (5, 10, 50, 100, and 500 μM), or probucol's vehicle (0.05% DMSO) for 3 d. Assayed for cell
493 viability (a), cell numbers (b), and cytotoxicity (c) were described under "Materials and methods". 0.1 μM
494 staurosporine (STS) was used as a cytotoxic-inducer control. Results were expressed as the mean \pm SEM
495 (n = 6). * $p < 0.05$ versus control.

496

497 **Fig. 2** Effects of probucol on apoptosis regulatory molecules and caspase-3 activity in PA-1 and
498 SKOV-3 cells. Total cell lysates from cells treated with 10% FBS (control), probucol (100 μM), vehicle, or
499 staurosporine (0.1 μM) for 3 d were subjected to Western blot analysis for Bcl-2 and cytochrome c (a),
500 Annexin V-FITC staining (c) and caspase-3 activity assay (d). Assayed for cytochrome c release in the
501 cytosolic fraction was described under "Materials and methods". Staurosporine (STS) was used as an
502 apoptotic-inducer control. (b) Laser densitometry of the gels showed in (a) and two additional experiments.
503 These are representative experiments, each performed at least three times in PA-1 and SKOV-3 cells. * $p <$
504 0.05 versus control.

505

506 **Fig. 3** Effects of probucol on protein levels of cdk4, cyclin D1, p21^{Waf1/Cip1}, p27^{Kip1}, c-Myc and PCNA in
507 PA-1 and SKOV-3 cells. Total cell lysates from cells treated with 10% FBS (control), probucol (100 μM),
508 or vehicle, for 12 h were subjected to Western blot analysis for cdk4, cyclin D1, p21^{Waf1/Cip1}, p27^{Kip1}, c-Myc
509 and PCNA (a). This is a representative experiment independently performed three times in PA-1 and
510 SKOV-3 cells. (b) Laser densitometry of the gels showed in (a) and two additional experiments. * $p < 0.05$
511 versus control.

512

513 **Fig. 4** Effects of probucol on cell cycle distribution in PA-1 and SKOV-3 cells. The cell pellets from
514 cells treated with 10% FBS (control), probucol (100 μM), or vehicle, for 24 h were fixed, stained, and

515 subjected to BD flow-cytometry systems for cell cycle distribution. This is a representative experiment
516 independently performed three times in PA-1 and SKOV-3 cells. * $p < 0.05$ versus control.

517

518 **Fig. 5** Effects of probucol on NF- κ B activation in PA-1 and SKOV-3 cells. Cytosolic or nuclear protein
519 from cells treated with 10% FBS (control), probucol (100 μ M), vehicle, or PDTC (10 μ M) for 12 h were
520 subjected to Western blot analysis for phospho-I κ B α (p-I κ B α), I κ B α , cytosolic p65 (C-p65), and nuclear
521 p65 (N-p65) (a). Histone H3 was used as an internal control for nuclear fraction. This is a representative
522 experiment independently performed three times in PA-1 and SKOV-3 cells. (b) Laser densitometry of the
523 gels showed in (a) and two additional experiments. * $p < 0.05$ versus control.

524

525 **Fig. 6** Effects of probucol on ERK/JNK/p38 MAPK activation in PA-1 and SKOV-3 cells. Total cell
526 lysates from cells treated with probucol (100 μ M), PD98059 (10 μ M), SP600125 (5 μ M), or SB203580 (5
527 μ M) in the presence of 10% FBS (control) for 12 h were subjected to Western blot analysis for
528 phospho-p42/p44 MAPK (a), phospho-JNK (b), and phospho-p38 MAPK (c) (upper panel) or proteins
529 corresponding to the above phosphorylated proteins (lower panel). This is a representative experiment
530 independently performed three times in PA-1 and SKOV-3 cells. * $p < 0.05$ versus control.

531

532 **Fig. 7** Effects of probucol, the NF- κ B inhibitor, and the ERK/JNK/p38 MAPK blockade on cellular
533 mitogenesis in PA-1 and SKOV-3 cells. Serum-deprived cells were treated with 10% FBS (control),
534 probucol (100 μ M), PDTC (10 μ M), PD98059 (10 μ M), SP600125 (5 μ M), SB203580 (5 μ M), probucol +
535 PDTC, probucol + PD98059, probucol + SP600125, or probucol + SB203580 in the presence of 10% FBS
536 (control) for 3 d. DMSO is the solvent used to dissolve the above kinase inhibitors. Assayed for cell
537 viability (a) and cell numbers (b) were described under "Materials and methods". Results were expressed
538 as the mean \pm SEM (n = 6). * $p < 0.05$ versus control; # $p < 0.05$ versus probucol.

539

540 **Fig. 8** Proposed effects of probucol on cell proliferation and apoptosis in human ovarian carcinoma. The
541 NF- κ B and ERK/JNK/p38 MAPK cascades are important growth factors/cytokines-induced signaling

542 pathways contributing to induction of cell proliferation in human ovarian cancer cells. Aberrant growth of
543 these cells can lead to ovarian carcinoma. In the presence of probucol, the activities of NF- κ B and
544 ERK/JNK/p38 MAPK were inhibited and the suppression of cell cycle progression was partly mediated by
545 enhancing p21^{Waf1/Cip1} and p27^{Kip1} but reducing cyclin D1 and PCNA. Nevertheless, probucol did not
546 induce apoptosis by modulating cytochrome c release and caspase-3 activity in human ovarian cancer
547 cells.
548

Figure 1

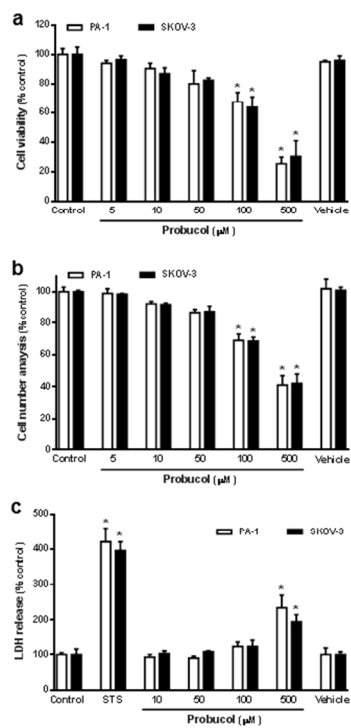
Figure 1
254x190mm (96 x 96 DPI)

Figure 2

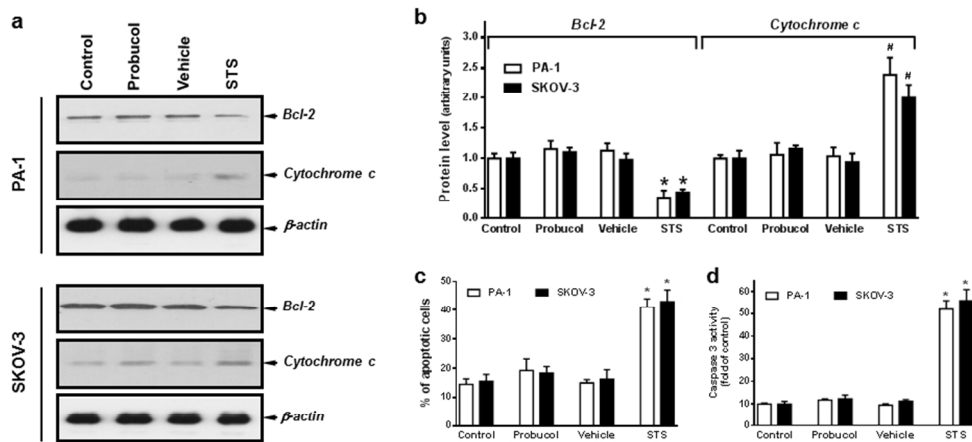


Figure 2
254x190mm (96 x 96 DPI)

Figure 3

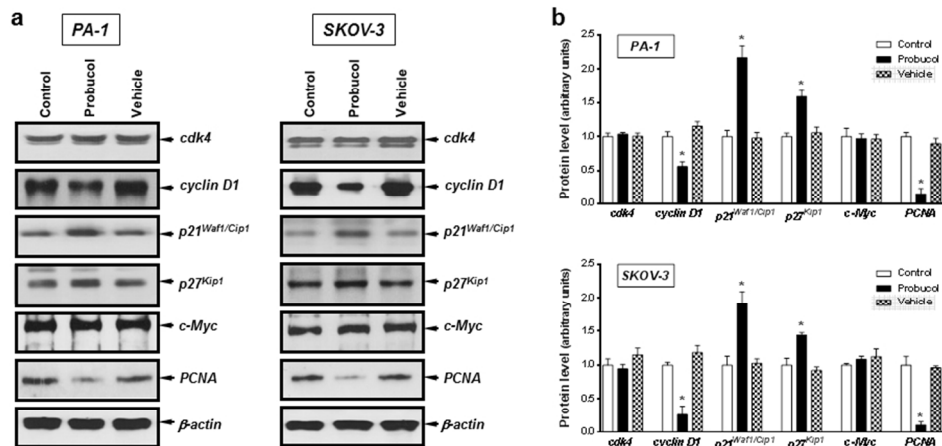


Figure 3
254x190mm (96 x 96 DPI)

Figure 4

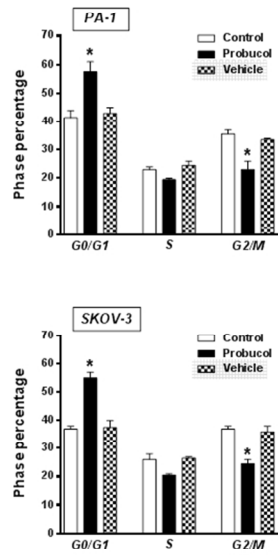


Figure 4
254x190mm (96 x 96 DPI)

Figure 5

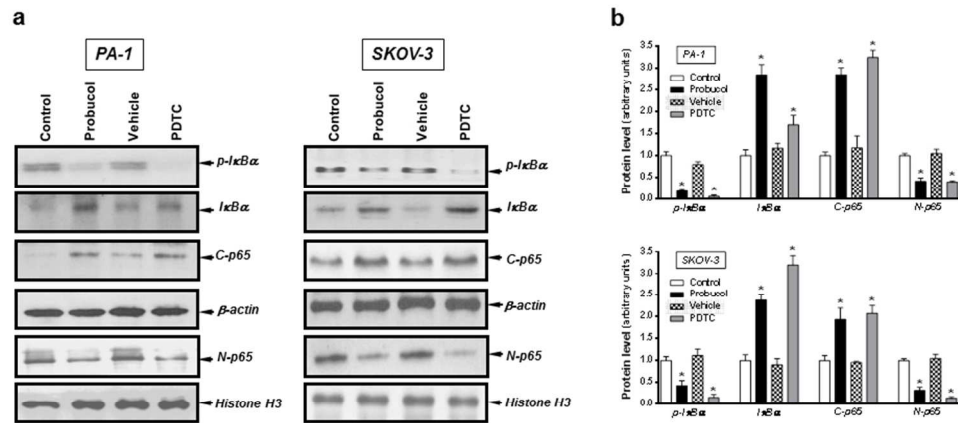


Figure 5
254x190mm (96 x 96 DPI)

Figure 6

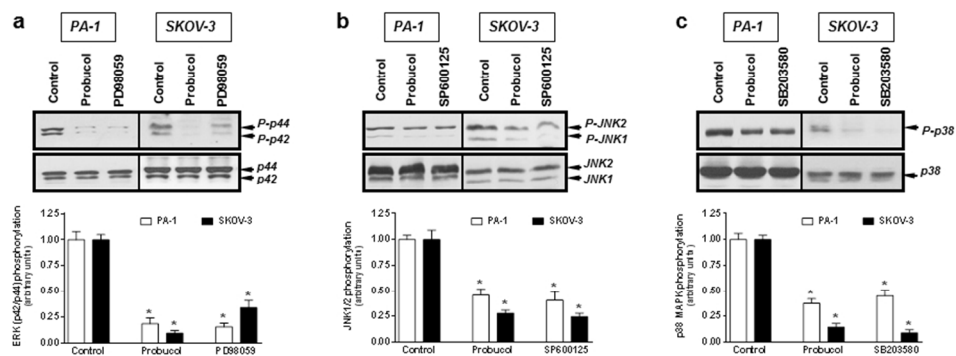


Figure 6
254x190mm (96 x 96 DPI)

Figure 7

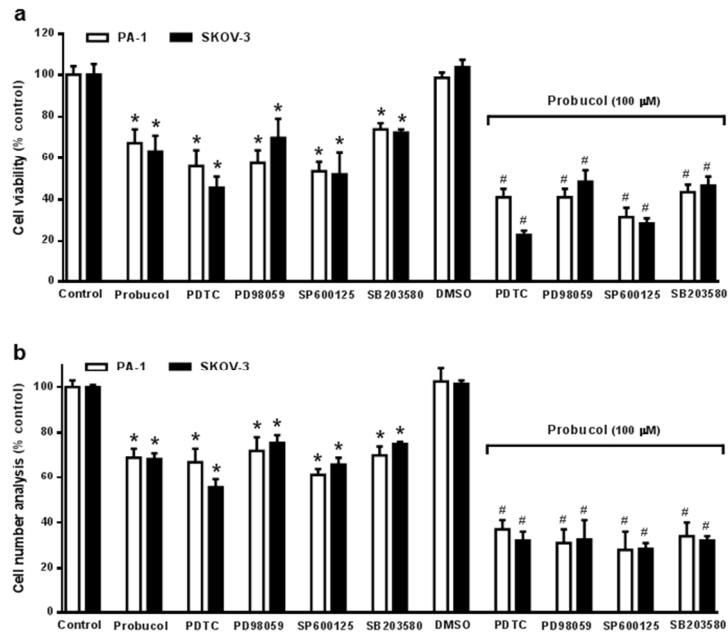


Figure 7
254x190mm (96 x 96 DPI)

Figure 8

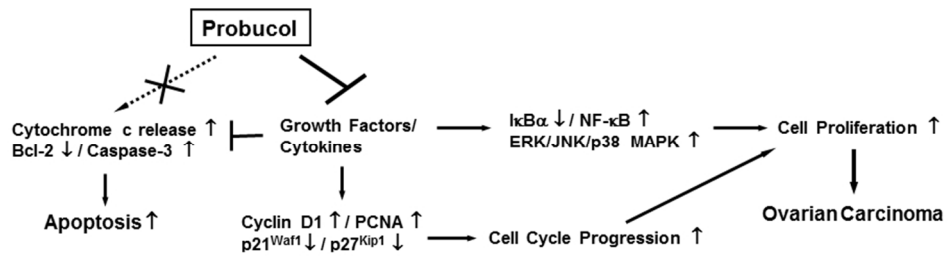


Figure 8
254x190mm (96 x 96 DPI)